Vol 17 No 5, May 2008
1674-1056/2008/17(05)/1645-07

Chinese Physics B

© 2008 Chin. Phys. Soc.
and IOP Publishing Ltd

Design and analysis of doped left-handed materials*

Zhang Hong-Xin(张洪欣)[a)†], Bao Yong-Fang(包永芳)[c)],
Lü Ying-Hua(吕英华)[b)], Chen Tian-Ming(陈天明)[a)], and Wang Hai-Xia(王海侠)[b)]

[a)] *School of Electronic Engineering, Beijing University of Posts and Telecommunications, Beijing* 100876, *China*
[b)] *Institute of Communication and Network Technology, Beijing University of Posts and Telecommunications, Beijing* 100876, *China*
[c)] *University of Electronic Science and Technology of China, Chengdu* 610054, *China*

(Received 13 August 2007; revised manuscript received 9 November 2007)

We devise three sorts of doped left-handed materials (DLHMs) by introducing inductors and capacitors into the traditional left-handed material (LHM) as heterogeneous elements. Some new properties are presented through finite-difference time-domain (FDTD) simulations. On the one hand, the resonance in the traditional LHM is weakened and the original pass band is narrowed by introducing inductors. On the other hand, the original pass band of the LHM can be shifted and a new pass band can be generated by introducing capacitors. When capacitors and inductors are introduced simultaneously, the resonance of traditional LHM is somewhat weakened and the number of original pass bands as well as its bandwidth can be changed.

Keywords: LHMs, doped materials, forbidden band, pass band
PACC: 0440, 1220, 1340, 2570E

1. Introduction

Materials exhibiting negative permittivity and permeability are popular topics of current researches due to their recent physical realization as metamaterials.[1−6] In 1998, Pendry *et al*[7] demonstrated that a thin continuous-metallic wire-array could have a first forbidden band from 0Hz up to a low plasma frequency in the GHz range, where the effective permittivity of the medium is negative. On the other hand, an array of split-ring resonators (SRRs)[8] can exhibit a negative effective permeability for frequencies close to the magnetic resonance frequency of these structures. By combining the SRRs and thin wires, Smith and Kroll[9] reported the first experimental demonstration of left-handed materials (LHMs). As proposed by Veselago,[10] one can observe negative Snell's law, reverse Doppler effect, and reverse Cerenkov radiation when electromagnetic (EM) waves propagate in these LHMs. To date, their imaginable applications extend to the field of antenna design, vehicle coatings for altering radar cross-section properties, and lenses.[11] However, current LHMs are designed with a small number of pass bands, and the controllability of these materials is not that desirable either.

This paper offers a fresh perspective on the transmission properties of three DLHMs: DLHM composed of LHM and doped inductors (LDLHM), DLHM composed of LHM and doped capacitors (CDLHM), and DLHM composed of LHM, inductors, and capacitors (LCDLHM). A numerical simulation on the SRR-only array is conducted first using the FDTD method, and the simulation result is then compared with Bayindir *et al*'s[12] measurement. Noting the good agreement of our simulation result with Bayindir's measurement, we then studied FDTD wave propagation in our designed media and find certain novel transmission properties. The DLHMs with inductors can narrow the LHM's pass bands and weaken the resonance of LHM; whereas DLHM with capacitors will shift the LHM's pass bands and result in new pass bands. And the DLHM with both inductors and capacitors displays a weakened resonance, a shifted pass band, and a new generated pass band.

2. Split-ring resonators

We first perform a numerical simulation for the SRR array constructed by Bayindir *et al.*[12] The pa-

*Project supported by the National Natural Science Foundation of China (Grant Nos 60671055 and 60771060) and Specialized Research Fund for the Doctoral Program of Higher Education of China (Grant Nos 20070013002 and 20070013004).
†Corresponding author. E-mail: hongxinzhang@263.net

rameters of the SRR structure are shown in Fig.1(a). The SRR in this experiment consists of two rings separated by a gap, both having splits at opposite sides. Figure 1(b) presents the metamaterial composed of periodically arranged boards which have SRRs on them. The thickness and the dielectric constant of the board are 0.45 mm and $\varepsilon_{\rm b} = 4.4$, respectively. Bayindir *et al*[12] have measured the response of EM waves to this metamaterial structure, which is made by $N_x = 25$, $N_y = 25$, and $N_z = 25$ unit cells. Each unit cell includes one SRR and the dimensions of the unit cell are $a_x = 5$ mm, $a_y = 3.63$ mm, and $a_z = 6$ mm. Their measurement was performed in free space by using HP 8510C network analyser and microwave horn antennas. For the measurement, the directions of the wave vectors, the incident electric field polarization and the magnetic field polarization are the same as those shown in Fig.1(a). Figure 2 shows that the SRR array exhibits a forbidden band between 8.7 and 10.2 GHz.

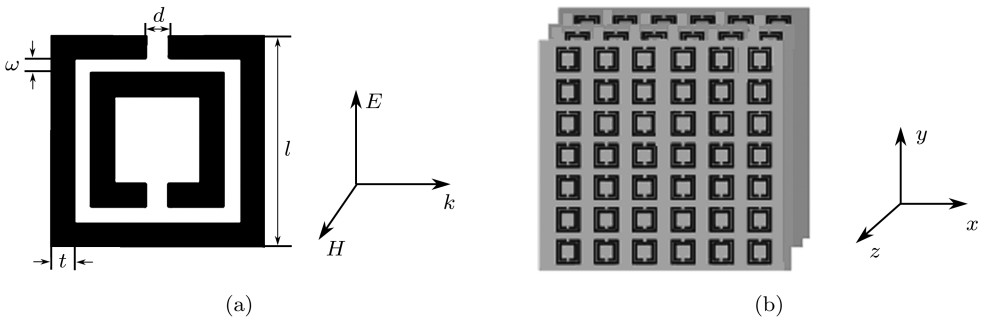


Fig.1. The unit cell of the SRR array with parameters $d = w = t = 0.33$ mm, $l = 3$ mm, and thickness of the SRR is 30 μm. The directions of incident electric and magnetic polarization are shown. (b) Schematic drawing of the configuration of the composite metamaterial consisting of SRRs.

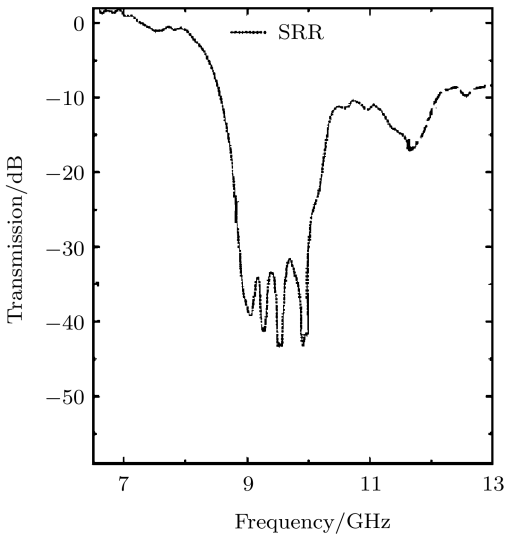


Fig.2. Measured transmission spectrum of the SRRs constructed by Bayindir.[12]

Our numerical simulation is based on the FDTD method. In the FDTD simulation, unit cells are of the same size as those in the measurement. We have considered 25 unit cells along the propagation direction and assumed periodic boundary conditions in the directions parallel to the interfaces. Figure 3 shows the calculated transmission spectrum of the SRR array. The SRRs give rise to a forbidden band from 8.7 to 9.4 GHz, which is in good agreement with Bayindir's measurement.

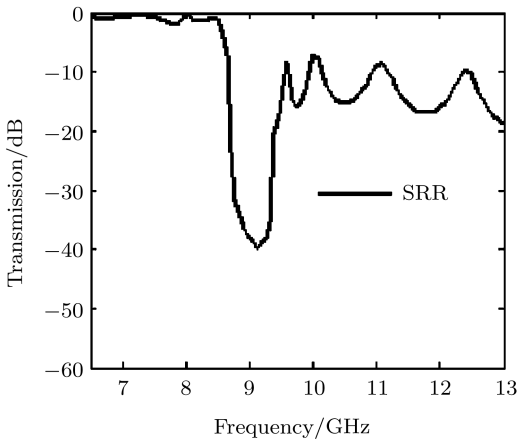


Fig.3. Calculated transmission of EM waves through an array of SRRs. The SRR array is formed according to Bayindir's structure.

3. Doped LHM

Three kinds of DLHMs are discussed here. These DLHMs are LDLHM, CDLHM, and LCDLHM. The wire arrays and the SRR arrays in all the following simulations share the same configuration. The metallic wires are continuous ones and their width and thickness are 0.3 mm and 30 μm, respectively. On the other hand, the SRR structure is also 30 μm thick. The dielectric constant of the boards is $\varepsilon_{\rm b} = 4.41$ and all the boards are 21.6 mm long in the propagation direction. Figure 4 shows the detailed parameters of our structure. In the following simulations, EM waves propagate along the x axis and the electric field polarization aligned along the y axis, whereas the magnetic field polarization is parallel to the z axis. The perfectly matched layer (PML) absorbing boundary condition is considered in the x direction while periodic boundary conditions are assumed in the y and z directions. Two neighbouring boards are 2.1 mm away from each other in the z direction. The dimensions of each grid in the FDTD simulation are $a_x = a_y = a_z = 0.3$ mm. Besides, the inductors and capacitors used as heterogeneous elements are lumped elements in the FDTD simulations.

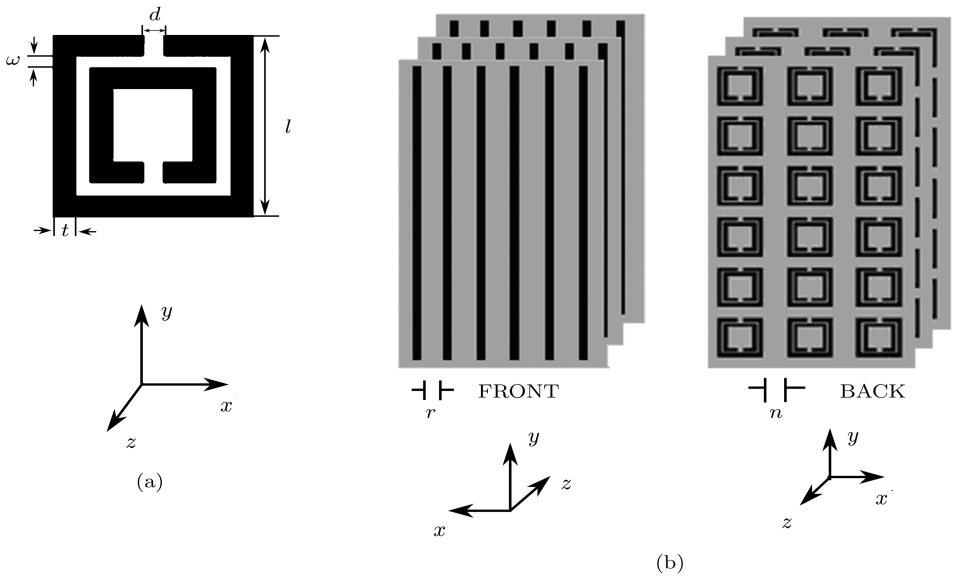


Fig.4. (a) The unit cell of the SRR array with parameters $d = w = t = 0.3$ mm and $l = 5.1$ mm. (b) Two sides of the board with the wire array and the SRR array. The distance between two neighbouring wires is $r = 3.3$ mm and the distance between two neighbouring SRRs is $n = 2.1$ mm.

3.1. Traditional LHM

We first give a description of the transmission properties of the traditional LHM constructed according to the configuration shown in Fig.4. In our simulations, the traditional LHM consists of the SRR-only array and the wire-only array. Figure 5 represents the calculated transmission spectra of the traditional LHM, the SRR-only array, and the wire-only array. One resonance at 4.3 GHz and a pass band from 8.2 to 10.5 GHz are presented in the transmission spectrum of the LHM because of the interaction between the SRR-only array and the wire-only array. This phenomenon can be similarly explained by the experiment conducted by Moss *et al.*[13]

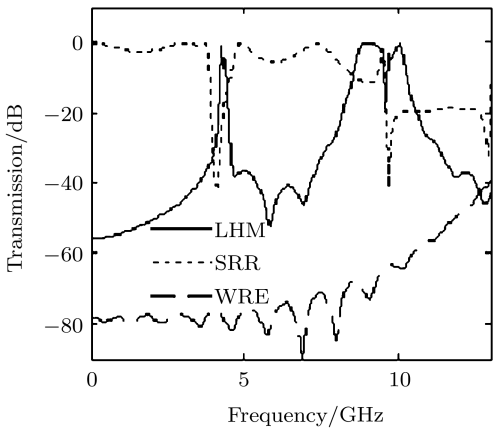


Fig.5. Calculated transmission spectra of the LHM, the CRR, and the SRR structure.

3.2. LHM doped with inductors (LDLHM)

We have fabricated this sort of DLHM by placing three rows of continuous inductors along the propagation direction and these inductors are on the surface where SRRs are located. The value of each inductor is $L = 1\,\mathrm{nH}$. However, there is no change for the wires on the other side of the board. Figure 6 gives us a closer look at this doped metamaterial. As can be seen, the inductors are continuous along the y axis. The distance from the left edge of the board to the nearest SRR is 0.6 mm and the distance between two neighbouring SRRs is 2.7 mm. While the distance from the right edge of the board to the nearest row of inductors is 0.6 mm and the distance between the two rows of inductors is 7.2 mm.

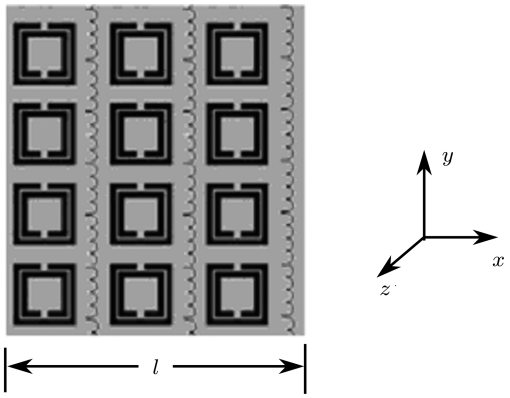


Fig.6. Three columns of continuous inductors embedded on the surface where SRRs are located. The board is 21.6mm long in the propagation direction.

Figure 7 shows the calculated transmission spectra of the traditional LHM, the inductor-only array, and the LDLHM. After inserting inductors as heterogeneous elements, we figure out that the transmission peak around 4.3 GHz is weakened and the original pass band from 8.2 to 10.5 GHz is shifted to a frequency range from 8.6 to 10.5 GHz. We think that these changes can be explained by the following facts. Continuous inductors have the capacitance between two neighbouring columns of inductors and have the performance of a high pass filter just like that of capacitors. Therefore, we observe a stop band starting from 0 Hz in the transmission spectrum of the inductor-only array. In this sense, the weakened resonance around 4.3 GHz is caused by the blocking effect of the introduced inductors in this frequency range. On the other hand, the Pendry wire array[5,6] plasma frequency is given by

$$f_{\mathrm{p}} = \frac{c}{a\sqrt{2\pi \ln\left(\frac{a}{r}\right)}}, \tag{1}$$

where a is the wire lattice spacing and r is the wire radius. It is well known that continuous wires can have a first forbidden band from 0 Hz to a low plasma frequency. Coupled to the negative permeability of SRRs, a resonance must appear in this forbidden band. The LHM's resonance in the forbidden band between 0 Hz and 8.2 GHz can be explained by this fact. Besides, as continuous inductors are inserted among continuous wires, the equivalent wire lattice spacing in Eq.(1) is decreased and the plasma frequency of LDLHM is increased. In this sense, we observe a resonance in an extended forbidden band as the plasma frequency of the doped medium is increased. Consequently, the original LHM's pass band from 8.2 to 10.5 GHz is narrowed after introducing these inductors.

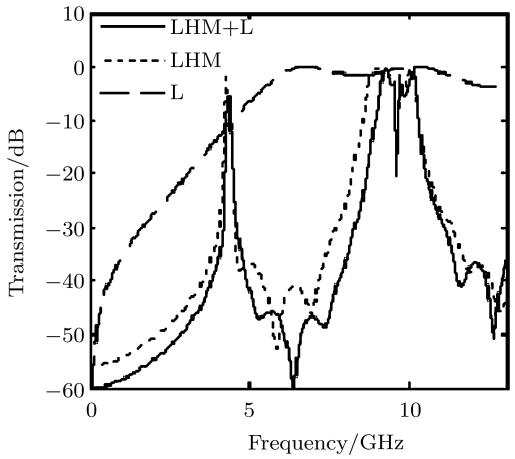


Fig.7. Calculated transmission spectra for the LHM, the inductor-only array, and the LDLHM.

3.3. LHM doped with capacitors (CDLHM)

The second sort of DLHM is constructed by inserting one group of continuous capacitors between two neighbouring rows of wires along the propagation direction. The SRRs on the other side of the board are unchanged and share the configuration shown in Fig.4. The value of each capacitor is $C = 1\,\mathrm{pF}$. The distance from the lower edge of the board to the nearest row of wire is 1.5 mm and the distance from the lower edge of the board to the nearest row of capaci-

tors is 3.3 mm. The front surface of each board composing this CDLHM is shown in Fig.8.

We have simulated EM waves propagate through this medium. The calculated transmission spectrum

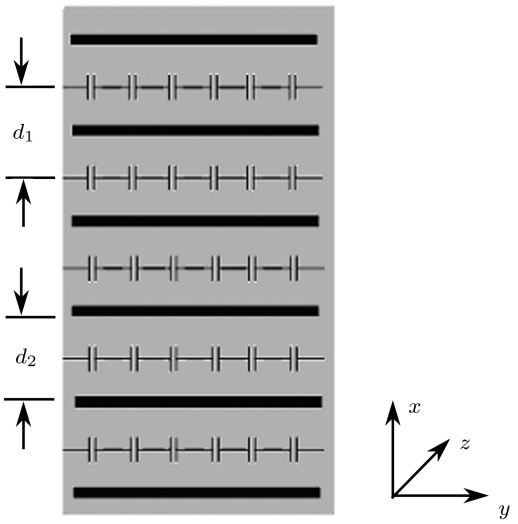


Fig.8. The front side of the CDLHM composed of wires, SRRs, and capacitors. The space between two neighbouring rows of capacitors is $d_1 = 3.6$ mm and the space between two neighbouring rows of wires is $d_2 = 3.6$ mm.

is shown in Fig.9. In contrast to the transmission spectrum of the traditional LHM, this CDLHM gives rise to a new pass band situated from 10.7 to 11.4 GHz. Moreover, the original pass band between 8.2 and 10.5 GHz is shifted to the frequency range from 7 to 9.6 GHz. These phenomena can be explained as follows. First, according to the quasi-static model proposed by Maslovski *et al*,[14] the plasma frequency for the wire array is given by

$$f_{\mathrm{p}} = \frac{1}{2\pi a\sqrt{\varepsilon_0 \varepsilon_{\mathrm{rave}} L}}, \tag{2}$$

where a is the wire lattice spacing and $\varepsilon_{\mathrm{rave}}$ is the average relative permittivity of a unit cell. L represents the wires' total inductance per unit length and is proportional to the magnetic flux ψ in a unit cell. The equivalent circuit model for a capacitor at microwave frequencies is a series L and C. As there are L components in the introduced capacitor structure, the magnetic flux ψ in a unit cell would increase substantially, and our new medium's total inductance per unit length is increased. Finally, the plasma frequency of the CDLHM is decreased. Besides, continuous wires can have a first forbidden band from 0 Hz to a low plasma frequency. Coupled to the negative permeability of SRRs, a resonance must appear in this forbidden band.[7] Therefore, we observe the original resonance around 4.3 GHz in a narrowed forbidden band from 0 Hz to a lower plasma frequency in the transmission spectrum of CDLHM. We think that the newly generated pass band ranging from 10.7 to 11.4 GHz is caused by the interaction between the inserted capacitors and the original LHM structure.

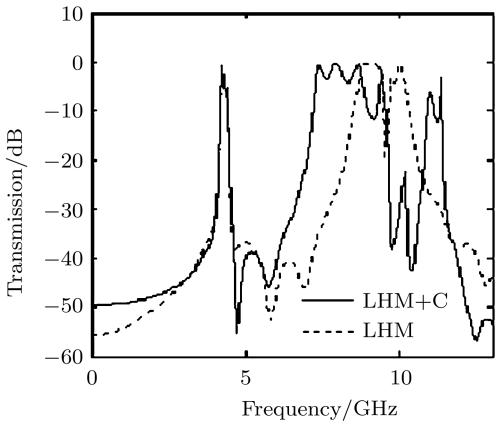


Fig.9. Calculated transmission spectra of the LHM and the CDLHM.

3.4. LHM doped with inductors and capacitors (LCDLHM)

We also devise a third sort of DLHM by combining the features of the LDLHM and CDLHM mentioned above. On the one hand, we insert one group of continuous capacitors between two neighbouring rows of wires along the propagation direction. On the other hand, we place three rows of continuous inductors along the propagation direction on the surface where SRRs are located. The value of each capacitor is $C = 1$ pF and the value of each inductor is $L = 1$ nH. Figure 10 depicts the two sides of each dielectric board comprising this LCDLHM. The configuration of the front side of the board is commensurate with that of the CDLHM, and the configuration of the back side of the board is commensurate with that of the LDLHM.

FDTD simulations then follow. The transmission spectrum of the LCDLHM is presented in Fig.11. The transmission peak around 4.3 GHz is weakened. According to our above discussions, the weakened transmission peak around 4.3 GHz can be explained by the blocking effect of the inductors in this frequency range. While, the forbidden band from 0 to 8.2 GHz is moved to lower frequencies but not as much as that in the transmission spectrum of the CDLHM. This is due

to the counteraction between the inductors and the capacitors. As shown in the transmission spectra of LDLHM and CDLHM, the inductors can increase the plasma frequency whereas capacitors can decrease the plasma frequency. In our simulations, the capacitors have more impact on the pass-band changes. As a result, the plasma frequency in this LCLHM has moved to a lower frequency and the change is not as much as that in the CDLHM. However, the new generated pass band between 11 GHz and 11.3 GHz can be traced to the interaction between the capacitors and the LHM structure.

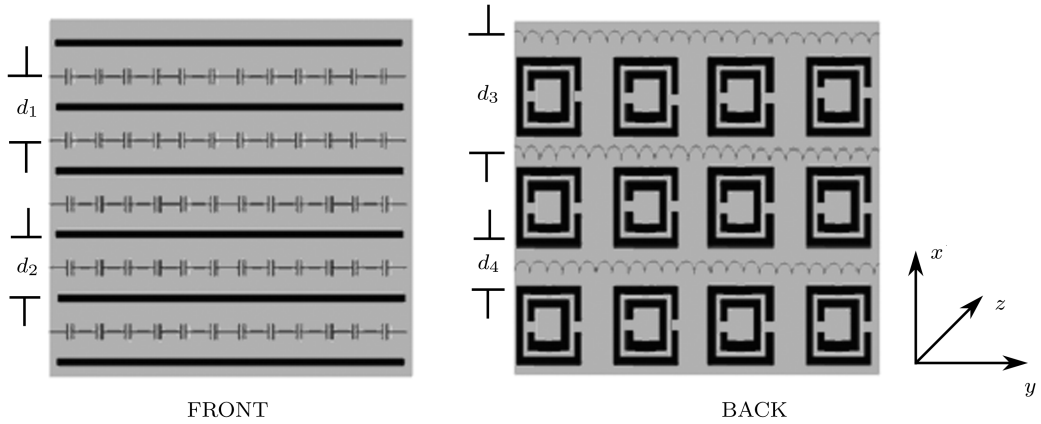


Fig.10. Two sides of each dielectric board. The space between two rows of capacitors is $d_1 = 3.6$ mm and the space between two rows of wires is $d_2 = 3.6$ mm. The distance between two rows of inductors is $d_3 = 7.2$ mm and the distance between every two SRRs is $d_4 = 2.1$ mm.

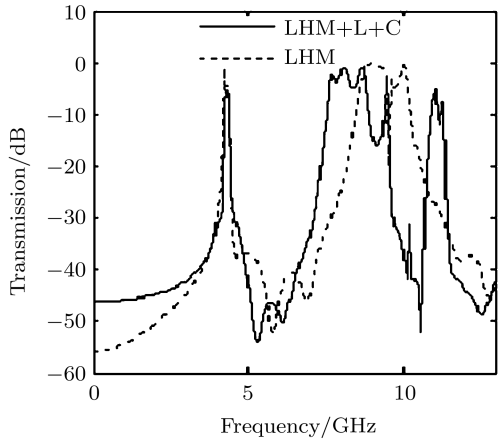


Fig.11. Calculated transmission spectra of the LHM and the LCDLHM.

4. Conclusion

In this paper, we have simulated the SRR structure devised by Bayindir and compared our calculation result with his measurement. Noting the good agreement between our simulation and the measurement, we then designed three sorts of DLHMs. In contrast to the traditional LHM we have measured, the LDLHM shows a weakened resonance in a wider forbidden band, whereas the CDLHM exhibits a shifted pass band with respect to the LHM and also gives rise to a new pass band. And the LCDLHM displays a weakened resonance, a shifted original pass band, and a newly generated pass band. We think that these unique features can be helpful in designing multi-pass-band filters with better controllability.

Acknowledgment

The authors specifically acknowledge the significant contributions of Dr Bao Yong-Fang. Dr Bao performed most of the initial development of the periodic-FDTD computer programs and our subsequent FDTD simulations of DLHMs are based on her original work.

References

[1] Smith D R, Padilla W J, Vier D C, Nemal-Nasser S C and Schultz S 2000 *Phys. Rev. Lett.* **84** 4184

[2] Shi H Y, Jiang Y Y, Sun X D, Guo R H and Zhao Y P 2005 *Chin. Phys.* **14** 1571

[3] Jiang T, Chen Y and Feng Y J 2006 *Chin. Phys.* **15** 1154

[4] Hu Y H, Fu X Q, Wen S C, Su W H and Fan D Y 2006 *Chin. Phys.* **15** 2970
[5] Zhang F L, Zhao Q, Liu Y H, Luo C R and Zhao X P 2004 *Chin. Phys. Lett.* **21** 1330
[6] Zhao Q, Zhao X P and Kang L 2004 *Acta Phys. Sin.* **53** 2206 (in Chinese)
[7] Pendry J B, Holden A J, Robbins D J and Stewart W J 1998 *J. Phys.* : *Condens. Matter* **10** 4785
[8] Pendry J B, Holden A J, Robbins D J and Stewart W J 1999 *IEEE Trans. Microwave Theory Tech.* **47** 2075
[9] Smith D R and Kroll N 2000 *Phys. Rev. Lett.* **85** 2933
[10] Veselago V G 1968 *Sov. Phys. Usp.* **10** 509
[11] Pendry J B 2000 *Phys. Rev. Lett.* **85** 3966
[12] Bayindir M, Aydin K, Ozbay E, Markos P and Soukoulis C M 2002 *Appl. Phys. Lett.* **81** 120
[13] Moss C D, Grzegorczyk T M, Zhang Y and Kong J A 2002 *PIER* **35** 315
[14] Maslovski S I, Tretyakov S A and Belov P A 2002 *Microwave Opt. Technol. Lett.* **35** 47